INSTITUTE OF PHYSICS PUBLISHING CLASSICAL AND QUANTUM GRAVITY

Class. Quantum Grav. **18** (2001) 2447–2456 www.iop.org/Journals/cq PII: S0264-9381(01)23595-3

Long-range tests of the equivalence principle

J D Anderson and J G Williams

Jet Propulsion Laboratory, California Institute of Technology, Pasadena, CA 91109-8099, USA

E-mail: john.d.anderson@jpl.nasa.gov and james.g.williams@jpl.nasa.gov

Received 8 December 2000

Abstract

The equivalence principle can be tested using accurate tracking of the Moon, planets, and interplanetary spacecraft. Tests with solar system bodies probe the dependence of the equivalence principle on self-energy. Analysis of lunar laser ranges yields the difference in the ratio of the gravitational and inertial masses for the Earth and Moon of $(-0.7 \pm 1.5) \times 10^{-13}$. In conjunction with laboratory tests of the equivalence principle and spacecraft and VLBI tests of PPN γ, one derives $|\beta - 1| \leqslant 0.0005$. Planetary tests are feasible, in particular tests using Mars. Improvements in Doppler accuracies under development may allow tests with interplanetary spacecraft.

PACS numbers: 0480, 0480C, 9510E, 9555P

1. Introduction

Long-range tests of the equivalence principle (EP) can utilize the Earth–Moon system, the planets, or interplanetary spacecraft. Analyses of laser ranges to the Moon have provided increasingly stringent limits on any EP violation, and a new solution is provided here. Future EP tests can analyse tracking data to determine the motion of a planet using landed or orbiting spacecraft, or the motion of spacecraft between planets.

2. Interplanetary tests

Evidence of a so-far undetected violation of the equivalence principle in the solar system could be detected if bodies which orbit the Sun fall at sufficiently different rates in the gravitational field of Jupiter [1]. The appropriate post-Newtonian equation of motion for a single orbiting body, including Newtonian gravitational perturbations from the eight major planets, but excluding the metric $(v/c)^2$ terms, which are not of concern here, is

$$\frac{\mathrm{d}^2\vec{r}}{\mathrm{d}t^2} = -\frac{\mu_s \vec{r}}{r^3} + \sum_{j=1}^{8} \mu_j \left[\frac{\vec{r}_j - \vec{r}}{|\vec{r}_j - \vec{r}|^3} - \frac{\vec{r}_j}{r_j^3} \right] - \eta \left(\frac{\Omega}{mc^2} \right)_s \sum_{j=1}^{8} \frac{\mu_j \vec{r}_j}{r_j^3}. \tag{1}$$

The two-body coefficient μ_s is the sum of Gm for the Sun and the body, the second term in equation (1) represents the Newtonian tidal perturbations from the eight planets with

$\mu_j = Gm_j$, the third term represents the acceleration produced by a violation of the EP, and all position vectors are Sun centred, with their magnitude given by $r_j = |\vec{r}_j|$. Because equation (1) contains the self-energy parameter η, which is zero in general relativity, it is not the most general form for an EP test. However, it can be generalized by replacing the Sun's normalized internal gravitational binding energy $(\Omega/mc^2)_s$ by the ratio of the Sun's gravitational mass to its inertial mass as demonstrated by Nordtvedt [2, 3].

$$\left(\frac{m_G}{m_I}\right)_s = 1 + \eta\left(\frac{\Omega}{mc^2}\right)_s. \tag{2}$$

As in all EP tests, this is a differential acceleration measurement, although we ignore the negligible difference from unity for the orbiting body's mass ratio m_G/m_I.

The normalized internal binding energy, or self-energy, for a homogeneous body is $-3/5(GM/c^2R)$. For a centrally condensed body, approximated by a point core overlain by an envelope of uniform density and mass M_e, the homogeneous value is multiplied by the factor $(\frac{5}{2} - 3M_e/2M)(M_e/M)$, which ranges from zero for a massless envelope, to $\frac{25}{24}$ for its maximum value at $M_e/M = \frac{5}{6}$, to unity at $M_e/M = 1$. The Sun's normalized binding energy is about -3.52×10^{-6}, and among the eight planets, the last term in equation (1) is dominated by Jupiter at 5.2 AU from the Sun, followed by Venus at 0.723 AU, Earth at 1.0 AU and Saturn at 9.54 AU, all three EP effects are smaller than Jupiter by factors of 7.5, 12 and 13, respectively. The lunar laser range (LLR) test limits the magnitude of η to 0.0002 ± 0.0008 (see section 3). With the acceleration from Jupiter (Gm_J/r^2) equal to 2.09×10^{-10} km s^{-2}, the corresponding limit on the magnitude of the EP acceleration in the direction Sun–Jupiter is $(1.5 \pm 6.0) \times 10^{-19}$ km s^{-2}. This acceleration limit for a possible binding energy effect holds for all interplanetary tests.

We have considered the sensitivity of spacecraft radio tracking from the Deep Space Network (DSN) to an acceleration this small, as well as the sensitivity of radio ranging data to landers on the Martian surface. Previously [1], we showed that 6 yr of Viking Lander data between 1976 and 1982, plus Mars Orbiter data from 1971, a range fix on Mars using the Russian Phobos spacecraft, and a month of data from the Mars Pathfinder Lander could reach the required sensitivity level, and could provide an independent test of the EP with comparable accuracy to the LLR result. However, the data analysis has not been done to date, although doing so could provide a test of the EP over planetary distances, as well as adding a four-body problem (Sun, Earth, Mars, Jupiter), with Jupiter providing the source of the gravitational field, to the LLR three-body problem (Sun, Earth, Moon), with the Sun providing the source of the gravitational field.

With regard to interplanetary spacecraft tracking data, the required EP sensitivity level for accelerations is not achievable at present. In effect, an interplanetary spacecraft is substituted for Mars, and the spacecraft is tracked in a drag-free environment for a decade or more. As for Mars, both ranging data and Doppler data are required (radio Doppler measures differential range to higher accuracy than an absolute radio range measurement, both data being useful for spacecraft orbit determination). Alternatively, Doppler data could be time differentiated in batches over days or months in order to obtain independent averages of acceleration at a sample interval equal to the batch interval. With this approach, the standard error σ_a for the reduced acceleration data is proportional to the Allan variance σ_y [4] for the fractional Doppler frequency $(y = \Delta\nu/\nu)$ at 1000 s integration time. The proportionality constant is roughly c/τ, where τ is the sample interval for the acceleration data. As a rule of thumb,

$$\sigma_a \sim \frac{c}{\tau}\sigma_y. \tag{3}$$

Until recently, all coherent DSN tracking for NASA missions, inclusive of the Galileo mission to Jupiter, was done at S-band (2.3 GHz), or at best S-band was transmitted from the ground and coherently transponded by the spacecraft at X-band (8.4 GHz), which resulted in an improvement over S-band two-way tracking by a factor of $2^{1/2}$ to 2, depending on the level of effort put into the data reduction [5]. The dominant error source by far was the spectral broadening of the radio carrier frequency by interplanetary plasma, with a corresponding increase in Doppler noise. Currently, including the Cassini mission to Saturn and the Stardust mission to comet Wild 2, the standard tracking configuration is X-band transmitted and transponded, which because of the $1/\nu^2$ dispersive nature of interplanetary plasma noise, results in a factor of 10 improvement over S-band. For purposes of supporting Cassini radio science, including a Doppler gravitational wave search, the Cassini spacecraft and the DSN are also instrumented to take advantage of multi-link tracking at X- and Ka-band (32 GHz), which could in the future provide a factor of 100 improvement over the standard X-band configuration, again depending on the level of effort put into the data reduction, most importantly a tropospheric calibration of the data with water-vapour radiometry at the DSN stations. Without this calibration, the Earth's troposphere limits the Ka-band error to a factor no more than 10 times better than the X-band system. The Cassini configuration is scheduled to come on-line in April 2001, including the water-vapour radiometry. For now, until some experience is gained with this new system, the assumed Allan variance is $\sigma_y = 3.2 \times 10^{-16}$ for the coherent X- and Ka-band system, which can be compared with 3.2×10^{-13} for the older S-band system, and 3.2×10^{-14} for the current X-band system.

By a simple application of equation (3), together with the required acceleration sensitivity of 8×10^{-19} km s^{-2}, and with an Allan variance appropriate for the Cassini X- and Ka-band system, about 4 yr of drag-free Doppler tracking are needed before interplanetary spacecraft become competitive with Mars lander ranging and LLR data. Spacecraft tracking as a test of the EP is an experiment for the unforeseeable future.

A spacecraft orbiting or landed on a planet measures the motion of the planet. Because of their small masses, the motions of free-flying interplanetary spacecraft are subject to larger non-gravitational accelerations, such as radiation pressure or gas jet thrust, than are the motions of the planets or their natural satellites. If equivalence principle tests are to be extended to the largest variety of circumstances [6], the limitations on the accuracy of free-flying spacecraft need to be understood. The following two sections present two cases of anomalous spacecraft accelerations for which causes are not understood. Neither case matches expectations for an EP violation; for example, the directions of the anomalous accelerations do not match equation (1).

2.1. Pioneer spacecraft and long-range acceleration anomaly

An apparent anomalous, weak, long-range acceleration has been previously reported for the Pioneer 10 and 11 spacecraft on escape trajectories from the outer solar system [9–11]. A satisfactory fit to the S-band Doppler data requires the addition of a constant acceleration to the equations of motion with magnitude $(8.74 \pm 1.25) \times 10^{-13}$ km s^{-2}, directed towards the Sun. Shortly after it was reported, a number of explanations were offered. Two were serious enough for publication and for a reply. The first by Murphy [12] suggested that non-isotropic thermal emission from the spacecraft's instrument bay is the cause. The second by Katz [13] suggested that thermal emission from the back of the Pioneer spacecraft's high-gain antenna produces a radiation reaction force in the direction of the Sun, the heat input to the antenna coming from the radioisotope thermoelectric generators (RTG). These are both credible causes of systematic error, with about 70 W of thermal power needed in the anti-Sun direction (70 W/(Mc) $= 8 \times 10^{-13}$ km s^{-2}, with spacecraft mass $M = 295$ kg). However, our two

replies [14,15] showed that the power available is inadequate by at least a factor of six. Further studies have not changed our evaluation of thermal effects [11], in fact we are more confident of our replies than ever, but we agree that the systematic error is dominated by on-board forces, not by systematics generated external to the spacecraft or by computational systematics. The realistic total error from all sources is about 14% of the measured acceleration, a total error approximately equal to the thermal upper bound reported previously [14,15].

2.2. *Anomalous velocity increase at earth flyby*

The second spacecraft anomaly involves flybys of the Earth by the Galileo, NEAR and Cassini spacecraft. Earth flybys are an effective technique for increasing a spacecraft's heliocentric orbital velocity far beyond the capability of its propulsion system [16, 17], but the technique depends on the deflection of the geocentric trajectory, with the orbital energy per unit mass remaining constant (constant unperturbed hyperbolic velocity V_∞). However, for all three flybys an increase in the flyby velocity is required in order to fit the DSN Doppler and ranging data. This increase can be represented by a fictitious trajectory manoeuver at perigee, or it can be demonstrated by fitting the pre-encounter data, and subsequently using the resulting trajectory to predict the post-encounter data. The difference between the actual post-encounter data and the predicted data is consistent with the velocity increase determined from the fictitious manoeuver.

This anomalous trajectory behaviour was first noted shortly after the first Earth gravity assist for the Galileo spacecraft on 8 December 1990. Despite efforts by the Galileo navigation team and the Galileo radio science team to find a cause for this anomaly, none was found. Consequently, the Tracking and Data Relay Satellite (TDRS) was scheduled for the second Galileo Earth flyby 2 yr later on 8 December 1992. This time the perigee altitude was lower, 303 km versus 960 km, but unfortunately any anomalous velocity increase was masked by atmospheric drag. However, results were published for the two Galileo flybys as a possible anomalous space navigation result [18]. After the Earth flyby by the Near Earth Asteroid Rendezvous (NEAR) spacecraft on 23 January 1998, at an altitude of 539 km, the anomalous velocity increase was observed once again. Results were presented at a spaceflight conference [19], including a reanalysis of the two Galileo flybys, and with all three flybys based on the best Earth gravity field available in August 1998.

In summary, the Galileo anomalous increase in its hyperbolic excess velocity is $\Delta V_\infty = 3.92 \pm 0.08$ mm s^{-1} during its first Earth flyby in 1990, and the NEAR increase is $\Delta V_\infty = 13.46 \pm 0.13$ mm s^{-1} during its flyby in 1998. Yet another Earth flyby by the Cassini spacecraft on 18 August 1999 indicates a much smaller anomalous increase of $\Delta V_\infty \sim 0.11$ mm s^{-1}, although the data analysis is still in progress. The next Earth flyby occurred with the Stardust spacecraft on 15 January 2001, but the spacecraft was continuously jetting attitude-control gas. If this jetting can be modelled successfully, it may be possible to find a pattern in the velocity increase as a function of the hyperbolic flyby state at perigee, in particular the osculating values of V_∞ and eccentricity e. A possible $1/e^4$ dependence is shown in figure 1, determined from the three flybys analysed so far. Attempts to find this anomalous orbital energy increase for flybys of other planets have failed because the gravity fields are not known nearly as well as for the Earth, where a geopotential (EGM96) is available by anonymous FTP from NASA's Goddard Space Flight Center (GSFC). EGM96 is made up of harmonic coefficients, including their standard errors, complete through degree and order 360 [20], and covariances are included to degree and order 70. Perhaps in the future, the gravity fields for Venus and Mars, determined from orbiter data, could become sufficiently accurate that DSN Mars and Venus flyby data from earlier NASA missions could be used to search for an anomalous ΔV_∞. These old DSN

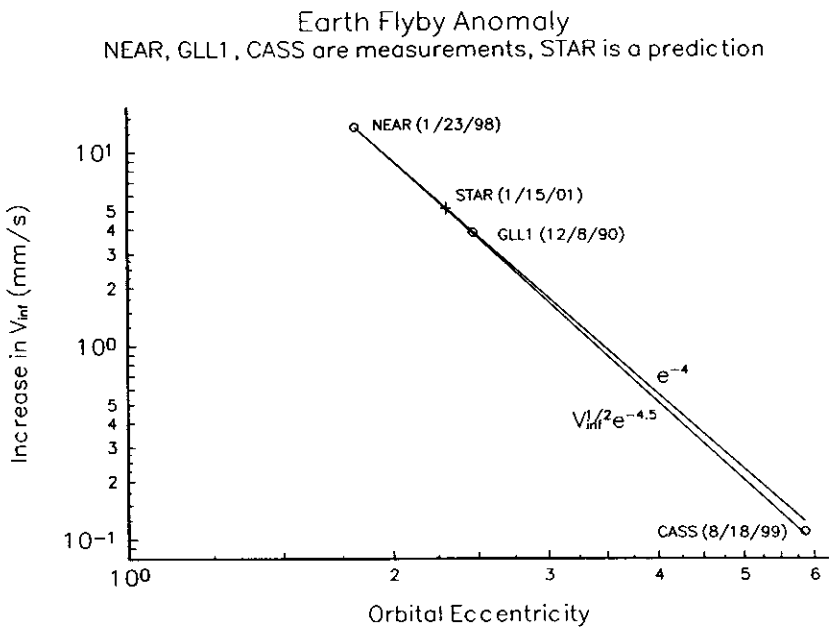

Figure 1. Values of anomalous ΔV_∞ for four Earth flybys by the Galileo (GLL), Near Earth Asteroid Rendezvous (NEAR), Cassini (CASS) and Stardust (STAR) spacecraft as a function of osculating eccentricity at perigee. The circles are the data and the plus is the prediction for Stardust data not yet analysed, given a trend proportional to e^{-4} for the other three analysed flybys. The lower curve represents an attempt to include V_∞ as part of a trend proportional to $V_\infty^{1/2}e^{-4.5}$. The closeness of the two curves indicates that it may be difficult to establish an empirical law for the anomalous orbital energy increase per unit mass. No clear pattern emerges when the total energy increase $mV_\infty\Delta V_\infty$ is plotted, the masses m being quite different for the three spacecraft, which suggests that ΔV_∞ is caused by anomalous gravity, not by an anomalous energy gain.

data can be retrieved from NASA's National Space Science Data Center (NSSDC) archive, where they were deposited by various radio science teams.

3. Lunar-laser ranging test

There are three decades of accurate laser ranges from three observatories on the Earth to four retroreflectors on the Moon. The McDonald MLRS and Observatoire de la Côte d'Azur/CERGA observing systems are operational, while Haleakala and the McDonald 2.7 m systems provided past data. The lunar retroreflectors are at the Apollo 11, 14 and 15 sites plus the Lunakhod 2 rover. The 14 235 laser ranges span March 1970 to July 2000. For the last 4 yr of ranges the weighted rms scatter after the fits is 1.6 cm. This scatter is 0.4×10^{-10} relative to the 385 000 km mean distance of the Moon.

The theoretical basis for the lunar test of the EP was established by Nordtvedt [21,22]. The first lunar laser tests were in 1976 [23,24]. A recent review of lunar laser ranging, including results for gravitational physics, is given by Dickey *et al* [25]. A later paper [26] is devoted to gravitational physics. Independent results are given by Müller and Nordtvedt [27]. The LLR EP results reported here improve on these published solutions by more than a factor of two. Recent solutions for gravitational-physics parameters, including the EP, are given in Williams *et al* [7].

3.1. Solutions

All fits of the lunar laser ranges involve a number of standard solution parameters for the Earth, Moon and lunar orbit (see [26] for the relativistic model used for JPL solutions). In this paper several separate least-squares solutions are discussed. A reference case involves the standard solution parameters. A second adds the EP. A third fixes the value of GM for the Earth plus Moon while solving for the EP.

The ephemeris for the Moon and planets plus the rotation of the Moon are generated by a simultaneous numerical integration. Least-squares solutions require partial derivatives of range with respect to all solution parameters. Partial derivatives for lunar orbit and rotation variations with respect to solution parameters are generated by numerical integration.

3.2. Equivalence principle solution

The LLR EP test depends on the relative acceleration of the Earth and Moon in the gravitational field of the Sun. A failure of the EP would polarize the lunar orbit along the Earth–Sun line [21,22]. The principal range signature has the 29.53 d mean synodic period of the new–full–new Moon cycle. The solution parameter is the ratio of gravitational to inertial mass M_G/M_I. The test is sensitive to the difference in M_G/M_I between the Earth and Moon.

The solution gives

$$\left(\frac{M_G}{M_I}\right)_{Earth} - \left(\frac{M_G}{M_I}\right)_{Moon} = (-0.7 \pm 1.5) \times 10^{-13}. \tag{4}$$

This solution is equivalent to a range variation of 2 ± 4 mm at the 29.53 d synodic period. The solution includes parameters for the GM of the Earth–Moon system and solid-body tidal displacements on the Moon. GM correlates with the EP by 0.34.

3.3. Equivalence principle implications

The LLR test is sensitive to EP violations, including violations due to composition and self-energy. A University of Washington EP laboratory experiment [28] is designed to simulate the compositional differences of the Earth and Moon. That test of the relative acceleration is $(0.1 \pm 3.2) \times 10^{-13}$. The laboratory results are insensitive to self-energy. A combination of the University of Washington composition test with the lunar laser result (equation (4)) yields the self-energy contribution to M_G/M_I,

$$\left(\frac{M_G}{M_I}\right)_{Earth} - \left(\frac{M_G}{M_I}\right)_{Moon} = (-0.8 \pm 3.5) \times 10^{-13}. \tag{5}$$

A combination using earlier LLR results is given in [28].

Tests for violations of the EP due to self-energy are sensitive to a linear combination of the parametrized post-Newtonian (PPN) quantities. Considering only the PPN parameters β and γ, we divide equation (5) by -4.45×10^{-10} to obtain

$$\eta = 4\beta - \gamma - 3 = 0.0002 \pm 0.0008. \tag{6}$$

This expression is null for general relativity, hence the small value is consistent with Einstein's theory.

The expression (6) is more sensitive to β than to γ. The parameter γ has been evaluated by other means, including Sun-induced time delay on interplanetary ranging and ray bending using VLBI (see [29] for a review, and for a definition of the PPN parameters). To date the published Viking Lander determination provides a verification that γ is unity to an uncertainty

of 0.002 [30]. By combining the Viking Lander determination of γ with the LLR determination of η (equation (6)), we obtain

$$|\beta - 1| \leqslant 0.000\,54. \tag{7}$$

A VLBI determination of $\gamma = 0.9996 \pm 0.0017$ [8], combined with the LLR result yields

$$\beta - 1 = -0.000\,05 \pm 0.000\,47. \tag{8}$$

In both cases the error on γ, not η, dominates the error on β.

3.4. Influences on present and future accuracies

The LLR-derived EP uncertainty depends on the range accuracy, modelling and fitting procedure. Recent range data are a factor of two more accurate than the best ranges used in Williams *et al* [26]. There have also been improvements in modelling, with major changes in the lunar rotation model [31]. Apart from the EP, gravitational influences on the lunar orbit at the 29.53 d synodic period are well constrained, and the non-gravitational solar radiation perturbation is 4 mm [32]. Several considerations are of particular interest to the lunar laser test of the EP.

There are a number of influences on the gathering of data which depend on, or correlate with, the phase of the Moon. Whether the target retroreflector is illuminated by sunlight or is in the dark determines:

(a) the amount of sunlight scattered back toward the observatory from the lunar surface;
(b) pointing technique, visual alignment when illuminated and offset pointing when dark; and
(c) solar heating and thermal effects on the retroreflector corner cubes.

Whether the observatory is experiencing daylight or night determines how much sunlight is scattered toward the detector by the atmosphere. As one approaches new Moon, the fraction of the time the Moon spends in the observatory's daylight sky increases, while the maximum elevation of the Moon in the night sky decreases (atmospheric degradation increases at low elevation).

The LLR data are non-uniformly distributed with respect to lunar phase. Figure 2 illustrates the distribution of observations in recent years versus angle D, the mean elongation of the Moon from the Sun, an approximation for lunar phase. There are no ranges near new Moon (0°) and few ranges near full Moon (180°). The operating observatories do not attempt ranging near new Moon, and only attempt full Moon ranges during eclipses. The non-flat distribution during much of the synodic month indicates that the efficiency of ranging changes with phase of the Moon.

A violation of the EP would cause an anomalous orbital displacement with a range signature proportional to $\cos D$. The cube root of GM of the Earth–Moon system scales the size of the lunar orbit. There is a major solar perturbation of the lunar orbit radius which depends on $\cos 2D$. It is also scaled according to the GM value. The Moon keeps one face toward the earth, but the direction to the Earth oscillates about 0.1 rad in the lunar sky (dominantly orbital 'optical libration', but some rotational 'physical libration'). So a retroreflector coordinate X, which is parallel to the principal axis in the mean Earth direction, projects along the orbit radius in proportion to the cosine of the libration. The observatory is displaced from the centre of the Earth and the reflector is on the Moon's surface, so the projection into range is modified by parallax. Tides raised on the Moon elongate the Moon along the Earth–Moon line and the tidal displacement depends on the Moon-centred angle between the retroreflector and Earth.

The projection of the X coordinate is nearly constant, so solutions with the LLR data give a high correlation between X and GM (or scale or semi-major axis). The $\cos 2D$

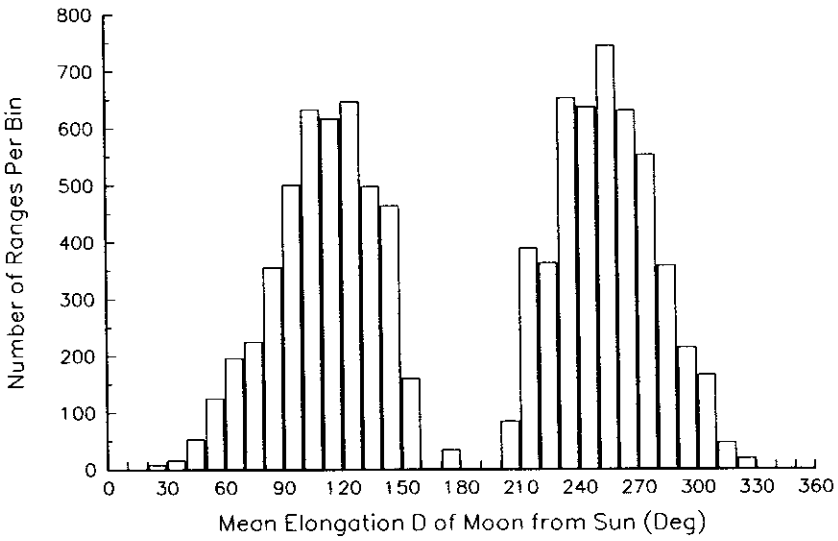

Figure 2. Distribution of lunar laser range observations versus angle D, the mean elongation of the Moon from the Sun. D is an approximation for lunar phase and $D = 0$ is near new Moon. The bins are 10° wide.

perturbation (period 14.765 d) promotes separation of scale and X. The uneven distribution of observations versus D causes the EP ($\cos D$) to correlate with GM (scale and $\cos 2D$) and X (cos(libration)). Nordtvedt [33] has simulated the three-parameter case with constant, $\cos D$ and $\cos 2D$ parameters. More generally, the time-varying projection of X along the Earth–Moon line is dominated by two half-month periodicities (13.777 and 13.606 d), so this helps reduce the correlations. The parallax effect, which depends on both the hour angle of the Moon as seen by the observatory and the libration angle, also reduces the correlations. Hour angle variation can be more than 180° for the Moon north of the equator and less south, but the fraction in daylight increases toward new Moon. Together these effects cause the 0.34 correlation between GM and the EP result, equation (4).

Tides on the Moon are of interest to the EP test. Among the periodicities is one involving $\cos 2D$. The tidal displacements depend on two Love numbers, h_2 and ℓ_2. In the solution leading to equation (4), h_2 is a weakly determined solution parameter, and the constraint $\ell_2 = 0.3h_2$, which is expected for a homogeneous elastic sphere, is imposed. In the solution leading to equation (4), h_2 has a low correlation with the EP, but it has a high correlation of -0.78 with GM. However, in a solution in which GM is fixed, the correlation between tides and the EP becomes higher (0.53) and the result of equation (4), including the uncertainty, is nearly duplicated. The tides contribute significant uncertainty at half the synodic period. While LLR determines the Love number k_2 in the lunar gravitational potential more accurately than the tidal displacement numbers, it is thought that the k_2 determination is biased by fluid core effects [25]. In the future, with an appropriate lunar core model, it may be possible to use the more accurate k_2 parameter to constrain h_2 and ℓ_2. Accurate determination of all of the lunar Love numbers depends on ranges to multiple reflectors.

Good distributions of observations versus lunar phase, semimonthly lunar orbit arguments, hour angle and various reflector locations all benefit the accuracy of the lunar laser EP test. Improved range accuracy will always translate into improved solution uncertainties.

4. Summary

Solar system bodies provide opportunities for tests of the EP. For interplanetary tests, spacecraft anchored to a planet would work well, for example landers on Mars. Spacecraft flying between the planets are more vulnerable to non-gravitational accelerations, but a drag-free spacecraft tracked with high-accuracy Doppler has possibilities.

Uncertainty in the lunar laser test of the EP has shrunk due to improved range accuracy, longer data span and an improved modelling and solution procedure. Compared with Williams *et al* [26], the accuracy of the test for the EP (equation (4)) is improved by a factor of three. Additional lunar range data will allow further improvements in tests of gravitational theory. In conjunction with improved composition-dependent tests of the EP, the self-energy dependence can be refined further.

Acknowledgments

We acknowledge and thank the staff of the CERGA, Haleakala and University of Texas McDonald Observatories, and the LLR associates. D H Boggs participated in the LLR solutions and E L Lau in the Cassini solutions. JDA thanks P G Antreasian, J R Guinn, E L Lau, M M Nieto and S Turyshev for their preliminary results on the Earth flyby anomaly. JDA acknowledges partial support as a Visiting Research Scientist, Monash University, Australia, under a Large Grant by the Australian Research Council. This work was performed at the Jet Propulsion Laboratory, California Institute of Technology, under contract with the National Aeronautics and Space Administration.

References

[1] Anderson J D, Gross M, Nordtvedt K L and Turyshev S G 1996 *Astrophys. J.* **459** 365–70
[2] Nordtvedt K 1968a *Phys. Rev.* **169** 1014–16
[3] Nordtvedt K 1968b *Phys. Rev.* **169** 1017–25
[4] Iess L, Giampieri G, Anderson J D and Bertotti B 1999 *Class. Quantum Grav.* **16** 1487–502
[5] Hellings R W, Callahan P S, Anderson J D and Moffet A T 1981 *Phys. Rev.* D **23** 844–51
[6] Overduin J M 2000 *Phys. Rev.* D **62** 102001-1–8
[7] Williams J G, Boggs D H and Dickey D O 2001 *Proc. 9th Marcel Grossman Meeting* (Singapore: World Scientific) at press
[8] Lebach D E, Corey B E, Shapiro I I, Ratner M I, Webber J C, Rogers A E E, Davis J L and Herring T A 1995 *Phys. Rev. Lett.* **75** 1439–42
[9] Anderson J D, Laing P A, Lau E L, Liu A S, Nieto M M and Turyshev S G 1998 *Phys. Rev. Lett.* **81** 2858–61
[10] Turyshev S G, Anderson J D, Laing P A, Lau E L, Liu A S and Nieto M M 2000 Gravitational waves and experimental gravity *Proc. 18th Moriond Workshop* ed J Dumarchez and J Tran Thanh Van (Hanoi: World) p 481
[11] Anderson J D, Laing P A, Lau E L, Liu A S, Nieto M M N and Turyshev S G 2001 *Preprint* gr-qc/0104064
[12] Murphy E M 1999 *Phys. Rev. Lett.* **83** 1890
[13] Katz J I 1999 *Phys. Rev. Lett.* **83** 1892
[14] Anderson J D, Laing P A, Lau E L, Liu A S, Nieto M M and Turyshev S G 1999 *Phys. Rev. Lett.* **83** 1891
[15] Anderson J D, Laing P A, Lau E L, Liu A S, Nieto M M and Turyshev S G 1999 *Phys. Rev. Lett.* **83** 1893
[16] d'Amario L A, Bright L E and Wolf A A 1992 *Space Sci. Rev.* **60** 23–78
[17] Wiesel W E 1989 *Spaceflight Dynamics* (New York: McGraw-Hill)
[18] Edwards C *et al* 1994 Astrodynamics 1993 *Advances in the Astronautical Sciences* ed A K Misra *et al* (San Diego, CA: Univelt) p 1609
[19] Antreasian P G and Guinn J R 1998 *Astrodynamics Specialist Conf. and Exhibition* (Washington: AIAA) paper no 98–4287
[20] Lemoine F G *et al* 1997 Gravity, Geoid and Marine Geodesy *Int. Symp. no 117* ed J Segawa *et al* (Heidelberg: Springer) p 461

[21] Nordtvedt K 1968c *Phys. Rev.* **170** 1186–7
[22] Nordtvedt K 1970 *Icarus* **12** 91–100
[23] Williams J G *et al* 1976 *Phys. Rev. Lett.* **36** 551–4
[24] Shapiro I I, Counselman C C and King R W 1976 *Phys. Rev. Lett.* **36** 555–8
[25] Dickey J O *et al* 1994 *Science* **265** 482–90
[26] Williams J G, Newhall X X and Dickey J O 1996 *Phys. Rev.* D **53** 6730–9
[27] Müller J and Nordtvedt K 1998 *Phys. Rev.* D **58** 062001-1–13
[28] Baeßler S *et al* 1999 *Phys. Rev. Lett.* **83** 3585–8
[29] Will C M 1993 *Theory and Experiment in Gravitational Physics* revised edn (New York: Cambridge University Press)
[30] Reasenberg R D *et al* 1979 *Astrophys. J.* **234** L219–21
[31] Williams J G, Boggs D H, Yoder C F, Ratcliff J T and Dickey J O 2001 *J. Geophys. Res. Planets* to appear
[32] Vokrouhlicky D 1997 *Icarus* **126** 293–300
[33] Nordtvedt K 1998 *Class. Quantum Grav.* **15** 3363–81